frontiers in Materials

ORIGINAL RESEARCH
published: 18 October 2019
doi: 10.3389/fmats.2019.00259

Transparent TiO_2 and ZnO Thin Films on Glass for UV Protection of PV Modules

*Wilhelm Johansson[1], Albert Peralta[2], Bo Jonson[1], Srinivasan Anand[2], Lars Österlund[3] and Stefan Karlsson[4]**

[1] LNU Glass Group, Department of Built Environment and Energy Technology, Faculty of Technology, Linnaeus University, Växjö, Sweden, [2] Department of Applied Physics, School of Engineering Sciences, KTH Royal Institute of Technology, Kista, Sweden, [3] The Ångström Laboratory, Department of Engineering Sciences, Uppsala University, Uppsala, Sweden, [4] RISE Glass, Built Environment Division, RISE Research Institutes of Sweden, Växjö, Sweden

Failure of PV modules frequently occurs as a result of degradation of their encapsulation material by destructive UV radiation. Both the life expectancy and efficiency of PV modules can be improved by reducing the transmittance of the destructive UV radiation through the cover glass without compromising the transmittance in the visible wavelength region. In addition, if the absorbed UV photons can be down-shifted to wavelengths that can be more efficiently converted to electrical energy, an additional increase of the PV efficiency could be achieved. In this study we have investigated transparent ZnO and TiO_2 thin films deposited by spray pyrolysis on soda lime silicate float glass as functional layers on PV cover glass. The optical bandgap, UV-cutoff, UV-Vis transmittance, reflectivity (total and diffuse) and photoluminescence have been determined. The ZnO coating shifted the optical bandgap to longer wavelengths, resulting in a reduction of the transmittance of destructive UV radiation by up to ∼85%. Distinct photoluminescence peaks at 377 nm and at 640 nm were observed for one of the ZnO samples. The TiO_2 coated glasses also showed an increased UV cutoff, which resulted in a reduction of transmittance of destructive UV radiation by up to 75%. However, no photoluminescence peaks could be observed from the TiO_2 films with 325 nm excitation laser, which can be explained by the fact that only indirect interband transitions are accessible at this excitation wavelength. Deposition of both ZnO and TiO_2 coatings resulted in a reduction of the transmitted light convertible by PV modules, by up to 12.3 and 21.8%, respectively. The implication of the results is discussed in terms of lifetime expectancy and efficiency of PV modules.

Keywords: float glass, thin films, UV protection, photovoltaic modules, cover glass, transparent intelligence, solar energy materials, photoluminescence

OPEN ACCESS

Edited by:
Lothar Wondraczek, Friedrich Schiller University Jena, Germany

Reviewed by:
Martin Charles Wilding, Sheffield Hallam University, United Kingdom
Paul A. Bingham, Sheffield Hallam University, United Kingdom

***Correspondence:**
Stefan Karlsson
stefan.karlsson@ri.se

Specialty section:
This article was submitted to Glass Science, a section of the journal Frontiers in Materials

Received: *30 November 2018*
Accepted: *30 September 2019*
Published: *18 October 2019*

Citation:
Johansson W, Peralta A, Jonson B, Anand S, Österlund L and Karlsson S (2019) Transparent TiO_2 and ZnO Thin Films on Glass for UV Protection of PV Modules. Front. Mater. 6:259. doi: 10.3389/fmats.2019.00259

INTRODUCTION

To stabilize the global temperature and mitigate climate change, the emission of anthropogenic greenhouse gases will have to be greatly reduced. To make it possible, the energy sector will have to transfer from fossil energy to environmentally friendly and carbon neutral sources (IPCC, 2014). Solar energy exists in abundance. In roughly 90 min, the solar energy that reaches the earth equals the consumption of all human societies globally during one year (IEA, 2011). Only a fraction of this energy is captured today, and photovoltaic (PV)

modules account for a marginal part of the electricity production worldwide, around 1.8% at the end of 2016. In recent years, however, the sector has been growing exponentially at a rapid rate, which means that the ability to increase efficiency and lifespan of PV modules is interesting from an energy perspective (Masson et al., 2018). PV modules consist of a number of interconnected PV-cells, embedded in an encapsulant and a protective cover glass on the top. One of the issues facing the PV modules available today is the degradation of their encapsulant, which most often consists of EVA (ethylene vinyl acetate). It is damaged by UV radiation with wavelengths below 350 nm. The UV radiation makes the encapsulant degrade and acquire a yellow and eventually brown hue, which reduces the efficiency of the PV modules (Czanderna and Pern, 1996; Oliveira et al., 2018).

Developing the cover glass has become increasingly important as the share of cost for the cover glass is high (Burrows and Fthenakis, 2015). The cover glass (Brow and Schmitt, 2009; Deubener et al., 2009) has several important functionalities, e.g., providing optimal light capture, rigidity, mechanical protection, and chemical protection. Optimal light capture depends on the optical properties of the cover glass such as absorption and reflection. The latter comprises the largest part, about 8% for a typical flat glass, which can be minimized by employing antireflective coatings (Nielsen et al., 2014). Rigidity and mechanical protection are determined by the thickness, the elastic modulus and the strength of glass (Wondraczek et al., 2011), which for PV cover glass is conventionally thermally strengthened (Karlsson and Wondraczek, 2019). The strength of glass is lowered continuously in operation by handling, and it therefore also depends on the glass's scratch and crack resistance (Rouxel et al., 2014; Sundberg et al., 2019). The chemical protection is important and glass provides an excellent chemical protection where in principle the only weaknesses are the lamination (Kuitche et al., 2014) and the potential induced degradation (PID) (Oliveira et al., 2018).

The optical properties of flat glass (Bamford, 1982; Rubin, 1985) are affected by the presence of iron impurities in the glass melt as the iron in the glass increases the absorption of light in the glass in the UV-VIS region of the electromagnetic spectrum. Iron can be used as a colorant of glass, giving the glass a green tint (Volotinen et al., 2008). In some cases, this is a positive feature, e.g., when UV-protection is needed in beer and champagne bottles (Daneo et al., 2009). In other cases, as with PV-modules where transparency is coveted (Goodyear and Lindberg, 1980), the iron in the glass is considered as a contaminant. In these cases, low-iron glass, where measures have been taken to reduce the iron in the glass, is frequently used.

In the case of cover glass for PV modules, the trend has been to use low-iron glass to increase transmitted light (Deubener et al., 2009). A drawback to this type of glass is that a larger amount of high-energy UV radiation is transmitted, which is harmful to the encapsulation material EVA that is used in most PV modules today (Allsopp et al., 2018). When UV radiation below 350 nm reaches the PV module, both the semiconductor material (Osterwald et al., 2003) and the laminate (Kuitche et al., 2014; Oliveira et al., 2018) are degraded. The degradation of the EVA laminate is the major reason for the annual degradation of 0.6–2.5% (Jordan and Kurtz, 2013; Kuitche et al., 2014). As a result of the UV radiation, EVA degrades and loses some of its high transmissivity as it gets a yellow/brown hue and eventually starts to delaminate, letting moisture into the PV modules, which leads to failure of the PV module (Oliveira et al., 2018).

In the current study we have investigated float glass coated with ZnO and TiO_2 thin films by spray pyrolysis of organometallic compounds of zinc and titanium. We present a detailed characterization of their optical properties by means of UV-Vis and photoluminescence spectroscopy.

TABLE 1 | Composition of precursor solutions.

	Isopropanol (ml)	Zn $(acac)_2$ (g)	Ti-isopropoxide (ml)	Wt% metalorganic complex	Mol% metalorganic complex
Zn solution	150	0.62	–	0.5	0.12
Ti solution	100	–	2.5	3	0.64

TABLE 2 | Sample series, amount of solution sprayed in grams denoted according to this numbering Zn2, Zn3, … and Ti1, Ti2… etc.

Sample ID	1	2	3	4	5	6
Zn solution (g)	–	12	16	24	32	40
Ti solution (g)	2	4	6	8	12	18

MATERIALS AND METHODS

Thin film depositions were made by spray pyrolysis in a hot wall reactor employing the precursor solutions shown in **Table 1**. The solutions were heated to 70°C for 2 h. The thin films were deposited on the air surface of AGC Planibel Clearview float glass samples (size 50 mm × 50 mm × 3.89 mm), which is a conventional soda-lime silicate float glass. The samples were heated up to 500°C, after which they were sprayed with the metal organic solution using a Preval sprayer (paintbrush equipment driven by the carrier gases dimethyl ether, isobutene, and propane). The furnace hatch was temporarily opened, and the precursor was sprayed onto the glass surface, manually holding the sprayer about a decimeter from the substrate. Between each opening of the furnace hatch, the furnace temperature was set to 500°C, implying that all depositions were made between 485 and 515°C. After deposition, the temperature in the furnace was lowered in a controlled manner at a cooling rate of 0.5°C / min down to 300°C, after which the furnace was turned off and the samples were left to cool down to room temperature. A series of six coated glasses with different deposited quantities were produced. The amount of precursor solution sprayed onto every glass sample is shown in **Table 2**, and the denotation of each sample according to the numbering. We believe that the deposited coatings are thin (<100 nm), mostly amorphous for both ZnO (Kamata et al., 1994; Hosseinmardi et al., 2012; Villegas

et al., 2018) and TiO_2 (Okuya et al., 1999; Abou-Helal and Seeber, 2002). This will be discussed in section Change in Transmittance and Reflection and section Effect on Photoluminescence. The surface morphologies of the coatings were measured using a Dimension 3100 (Bruker) Atomic Force Microscopy (AFM) and the root-mean-square (RMS) roughness was determined.

UV-Vis Spectrophotometry

Transmittance, $T(\lambda)$, and reflectance, $R(\lambda)$, spectra were recorded in the wavelength range between 325 and 850 nm with a step resolution of 2.5 nm, employing a Lambda 950 double-beam UV/Vis/NIR spectrophotometer equipped with an integrating sphere and a Spectralon reflectance standard. Both total and diffuse reflectance, $R(\lambda)$, were measured with 8° incidence angle. The absorptance, $A(\lambda)$ is then obtained as

$$A(\lambda) = 1 - T(\lambda) - R(\lambda) \tag{1}$$

Instrument corrected values of $T(\lambda)$ and $R(\lambda)$ were used in Equation (1) (Roos, 1993). In order to estimate the fraction of blocked UV light and the solar spectrum weighted $T\%$ and $R\%$ data for given single values throughout the paper, we calculate a Figure of Merit (*FoM*). The solar spectrum AM 1.5 G-173 from NREL, $\phi_{AM\ 1.5\ G}(\lambda)$, is used as the solar light intensity distribution function, and the weighted average is between 320 and 350 nm for estimating UV blocking and between 350 and 1200 nm for estimating $T\%$ and $R\%$ as single values, according to

$$FoM \times 100(\%) = \frac{\int_{\lambda_0}^{\lambda} P(\lambda) \cdot \phi_{AM\ 1.5\ G}(\lambda) \cdot d\lambda}{\int_{\lambda_0}^{\lambda} \phi_{AM\ 1.5\ G}(\lambda) \cdot d\lambda} \tag{2}$$

where λ and λ_0 is the wavelength range that is evaluated and $P(\lambda)$ represents $T(\lambda)$ or $R(\lambda)$.

Photoluminescence

The photoluminescence of the ZnO- and TiO_2-coated samples was measured using a Renishaw Invia Raman microscope employing a 40× objective lens. The samples were irradiated with a He-Cd laser with a wavelength of 325 nm, and photoluminescence of wavelengths between 330 and 720 nm were recorded. The maximum effect of the laser was 6 mW, but 99 and 90% of the laser flux was filtered away for the ZnO and TiO_2 samples, respectively.

Energy calibration was performed by Raman spectroscopy on non-coated float glass with the same instrument settings. Prior to the measurements, the instrument was calibrated by measuring the 1,332 cm^{-1} peak of the diamond.

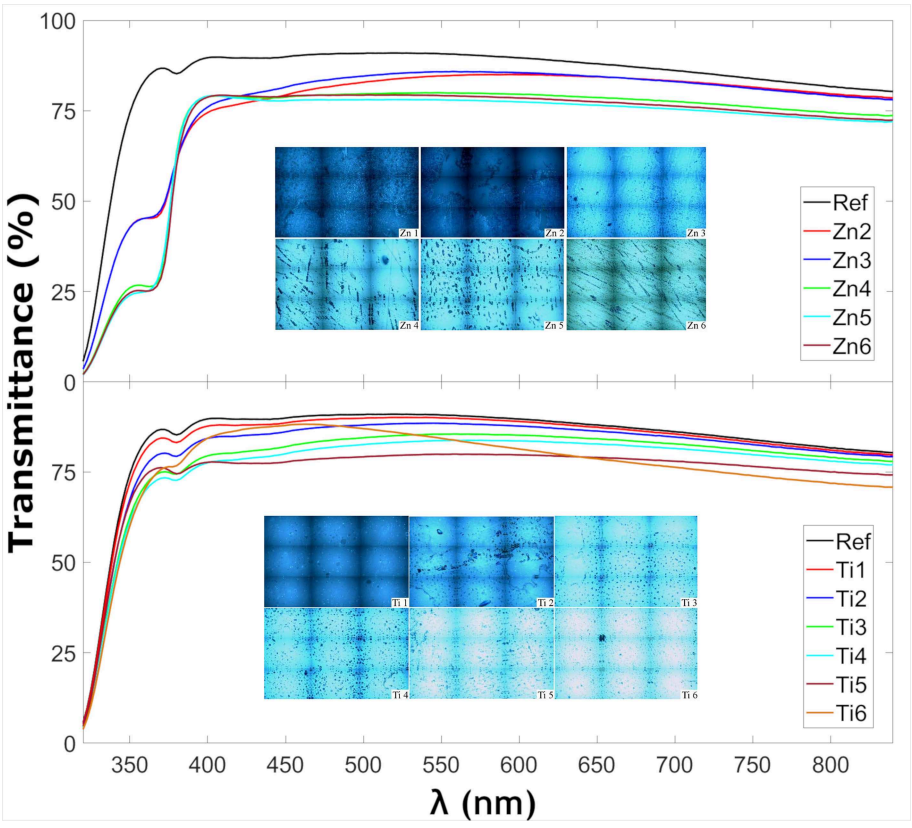

FIGURE 1 | Transmittance of thin film-coated glass samples at normal incidence as well as insets of microscope images of the samples taken from the Raman microscope.

TABLE 3 | Optical properties of coated glass samples, the fraction of the blocked UV light and the transmittance was calculated using (Equation 2).

Sample	Fraction of UV light blocked (%)[a]	Transmittance (%)[a]	Optical bandgap, E_g (eV)	UV cutoff wavelength (nm)[b]	RMS roughness (nm)
Estimated error	±2	±2	±0.01 (±2)	±2	±1
Reference	54.6	85.2	3.53 (351 nm)	322.7	0.5
Zn2	73.0	79.8	3.57 (347 nm)	325.6	31.0
Zn3	73.0	80.3	3.58 (346 nm)	325.6	4.2
Zn4	83.4	75.7	3.58 (346 nm)	329.6	8.4
Zn5	84.7	74.1	3.58 (346 nm)	330.0	8.0
Zn6	84.2	74.7	3.59 (345 nm)	330.4	8.0
Ti1	57.3	83.9	3.54 (350 nm)	323.0	2.0
Ti2	63.6	81.6	3.52 (352 nm)	323.6	2.7
Ti3	70.0	76.9	3.51 (353 nm)	324.1	5.4
Ti4	71.5	75.2	3.53 (351 nm)	324.2	4.4
Ti5	67.5	69.8	3.55 (349 nm)	323.6	11.6
Ti6	74.2	66.7	3.54 (350 nm)	324.8	4.8

Root-mean-square (RMS) data as determined from Atomic Force Microscopy (AFM).
[a]Defined as given in section UV-Vis spectrophotometry.
[b]Defined as given in section optical bandgap and UV cutoff wavelength.

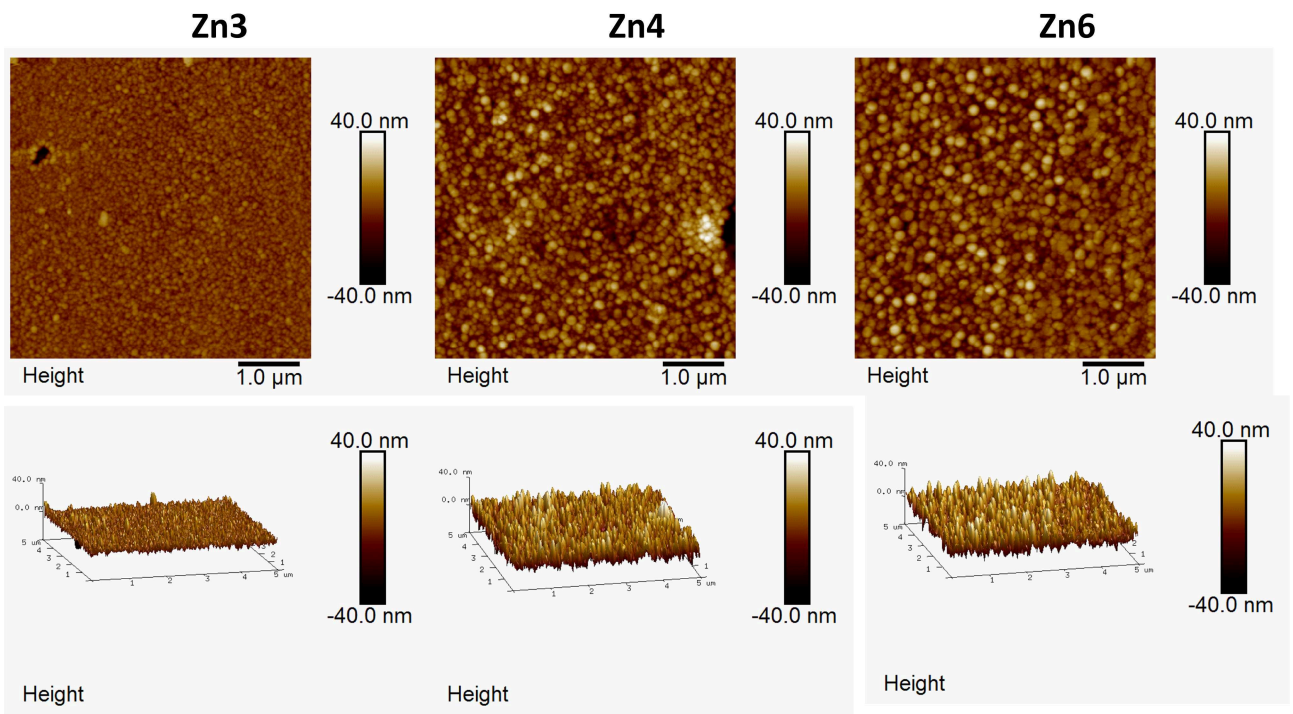

FIGURE 2 | 2D and 3D AFM images of selected ZnO-coated samples.

Optical Bandgap and UV Cutoff Wavelength

From the spectrophotometry data it is possible to estimate the optical bandgap, i.e., at which wavelength the coated glass starts to absorb most of the radiation acting as a short wavelength cutoff filter. In this study the cutoff wavelength was defined as the wavelength below which <10% of the incoming light is transmitted, i.e., at a somewhat larger wavelength compared to the optical bandgap.

The optical bandgap, E_g, of the coated glasses was analyzed according to a simplified demarcation point analysis which is very similar to the Tauc analysis (Tauc, 1968). The demarcation point can be graphically extracted from $A(\lambda)$ by approximating the bandgap region below E_g with a fairly horizontal straight line

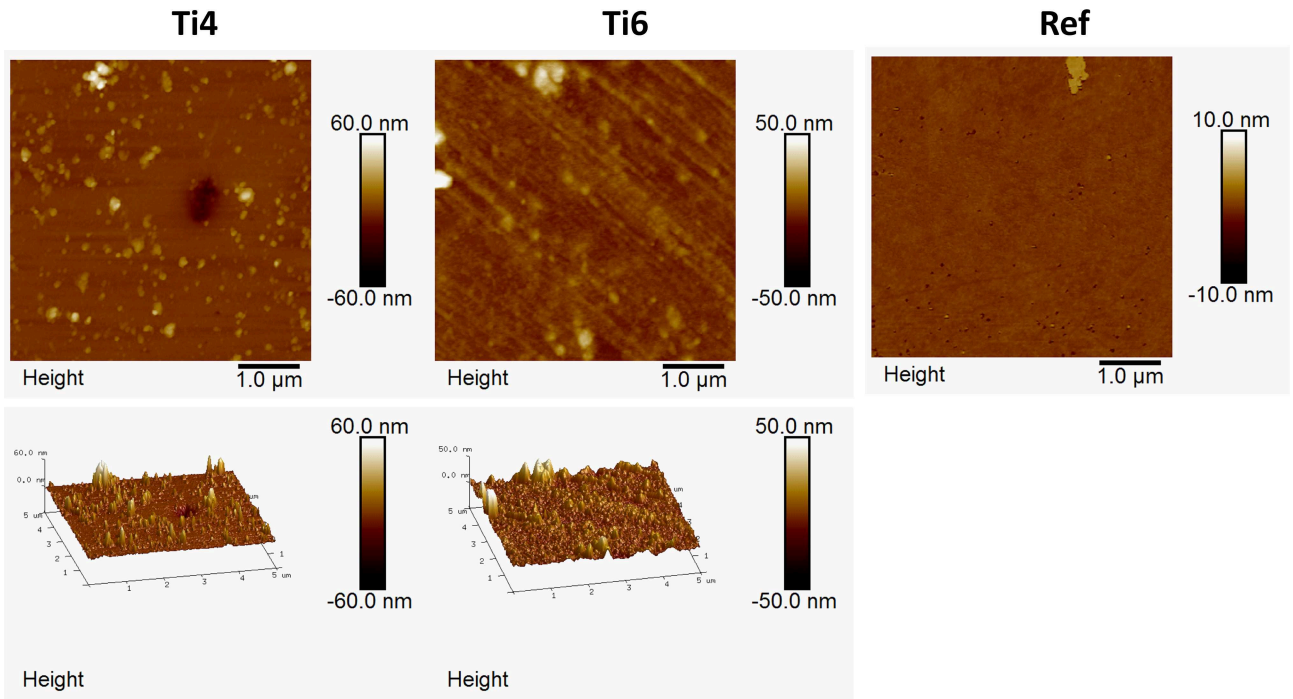

FIGURE 3 | 2D and 3D AFM images of selected TiO_2-coated samples.

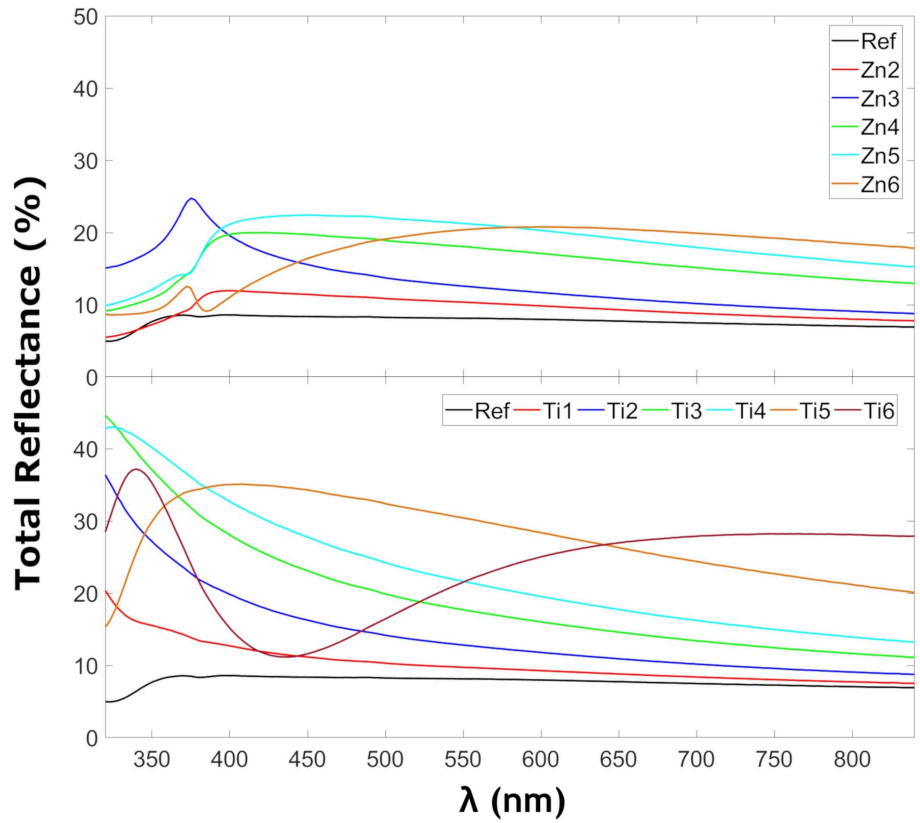

FIGURE 4 | Total reflectance of thin film-coated glass samples.

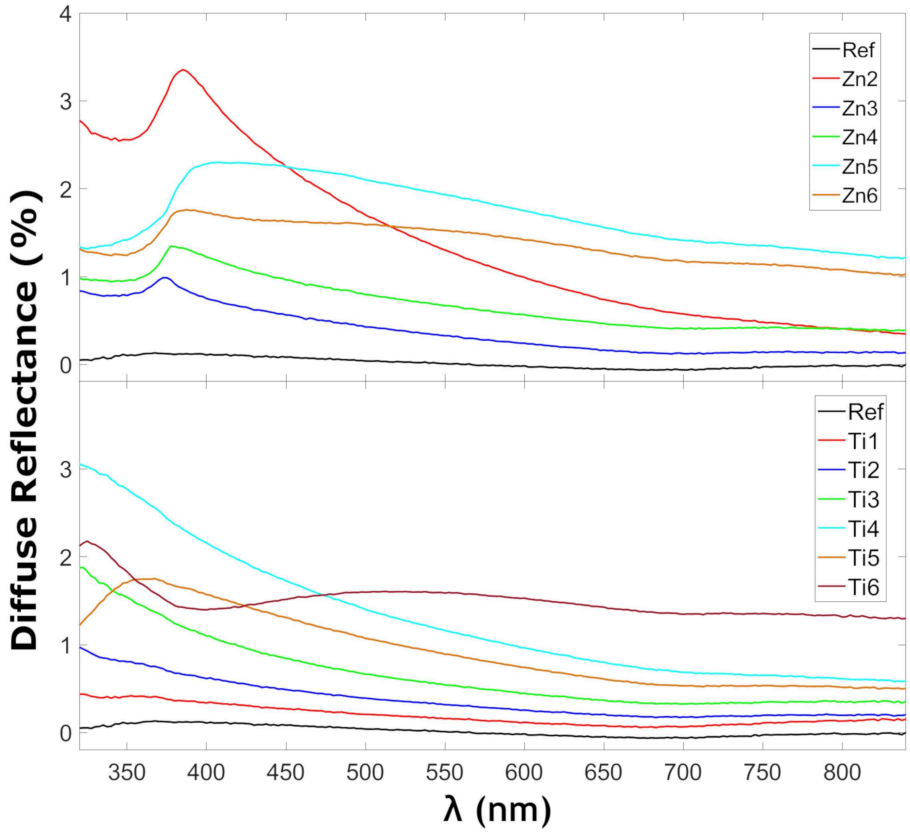

FIGURE 5 | Diffuse reflectance of thin film-coated glass samples.

and approximate the region above E_g (the actual UV-edge) with another straight line. The point where these two straight lines intersect is the demarcation point and is a good approximation of the E_g.

RESULTS

Change in Transmittance and Reflection

Figure 1 shows the transmittance at normal incidence for the glass samples coated with ZnO and TiO_2, respectively. The insets in **Figure 1** show optical microscopy images acquired with the Raman instrument, showing that the thin films consist of particulate features with a root-mean-square roughness of about 4–8 nm for the ZnO and 2–10 nm for the TiO_2 samples (see **Table 3**) which is quite common for the spray pyrolysis technique (Perednis and Gauckler, 2005). The ZnO coatings show the expected rough surface, see **Figure 2**. The highest roughness is for the thinnest layer, Zn2, while the others have comparable roughness values. In comparison, for the TiO_2 coated samples, see **Figure 3**, there are larger structures with peak to valley heights in the range 60–150 nm. Also, most samples show clear pits/openings in the film. The depths of these openings are in the range 10–40 nm. Both ZnO- and TiO_2-coated glass show a decrease of the transmittance compared to the uncoated reference sample. The ZnO-coated samples showed larger transmittance in the visible regime than the TiO_2-coated. While the sample coated with the largest amount of ZnO (sample Zn6) showed a transmittance of 74.7%, the transmittance for the sample coated with the largest amount of TiO_2 (sample Ti6) was 66.7%, see **Table 3**. Glass with ZnO coatings showed a decreased transmittance in the UV regime <350 nm, exhibiting a plateau between 320 and 370 nm. A small absorption peak can also be observed for the reference samples at 380 which can be denoted to tetrahedral configuration of Fe^{3+} (Volotinen et al., 2008). Therefore, we attribute the plateau between 320 and 370 nm for the ZnO-coated samples to be caused by Fe^{3+} but sensitized by the presence of ZnO thin film.

Figure 4 shows the reflectance in the glass samples coated with ZnO and TiO_2. The TiO_2 coated glasses show more reflection as expected due to a larger refractive index mismatch between the glass and the coating. The refractive index for TiO_2 is 2.65 for rutile-TiO_2 (Jellison et al., 1997) or 2.56 anatase-TiO_2 (Schröder, 1928) and for ZnO 2.0 (Jellison and Boatner, 1998), all reported at 589.3 nm as reported by Shannon et al. (2002). The peaks at 375 nm for the ZnO samples coincide with their observed absorption edge in **Figure 6** as expected for localized transitions, signaling the presence of defect states, possibly with contribution from Fe^{3+} charge transfer reactions, since the reference sample also exhibits small absorption in this region. It has only been

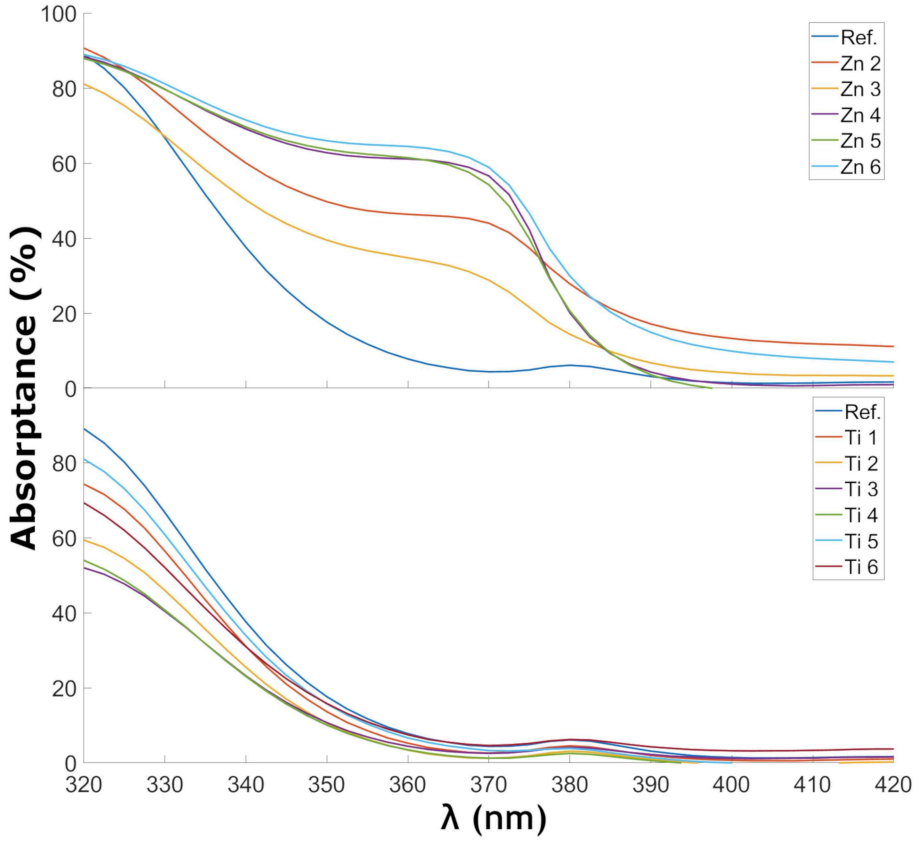

FIGURE 6 | Absorptance of ZnO- and TiO_2-coated glass samples in the wavelength range near the UV cutoff.

possible to find a zone without that reflection behavior for Zn5. That zone without the mentioned peak corresponded to a place which was far from the internal crack that the sample presented. It has been seen that the samples with that behavior show more spot to spot deviance in reflection measurements. **Figure 5** shows the diffuse reflection in the ZnO of the TiO_2-coated samples, respectively. The diffuse reflection of the coatings is <4% for both coatings. The low diffuse reflection is likely to be caused by non-uniform deposited thin films. This means that parts of the diffuse transmitted light that reaches the glass back end will be reflected back into the glass instead of being transmitted through it, similar to a conventional light trapping and back-reflecting cover glass structure (Deubener et al., 2009).

The measured transmittance/reflectance spectra do not exhibit any interference patterns as is expected for thin films with thicknesses >> 100 nm.

Change in UV-Cutoff and Optical Band Gap

Figure 6 shows the change in absorptance near the UV-cutoff in the glass samples coated with ZnO and TiO_2. A trend can be observed of a shift of the UV-cutoff to longer wavelength as more ZnO was deposited. This trend is less clear for TiO_2. The estimated optical bandgaps, using the demarcation point analysis, are shown in **Table 3**. In the ZnO spectra, two UV edges can be observed: one at about 330 to 340 nm and another one at 375 to 380 nm. The latter gave optical bandgap values in the range of 3.21–3.22, i.e., very similar to the wurtzite form of ZnO. The optical band gap of ZnO in wurtzite and zinc-blende form is 3.22 and 3.12 eV, respectively (Lee et al., 2002). The TiO_2-coated glasses also show a small absorption peak at 380 nm which is caused by the tetrahedral configuration of Fe^{3+} (Volotinen et al., 2008). TiO_2 in rutile, anatase, and brookite form has optical band gaps at 3.00, 3.21, and 3.13 eV, respectively (Dhar et al., 2013). The estimated optical bandgaps in **Table 3** are in the range around 3.55 eV, i.e., much influenced by the float glass and its conventional impurity Fe_2O_3. Fe_2O_3 has a considerable effect on the UV absorption and probably overshadows some of the effects that would otherwise be seen by our coatings (Volotinen et al., 2008). This is discussed more in section Discussion of the Effect for PV Modules.

UV-Blocking

Table 3 shows the UV-blocking characteristics as well as the transmittance of light convertible for Si-PV modules. The-ZnO coated samples show larger percentages of blocked UV light with larger transmission in the visible range compared with TiO_2 coatings. Compared to the reference float glass, the coatings show a relative increase of the *FoM* (c.f. Equation 2) up to 54.3 and 36.0% of UV-blocking characteristics and a relative decrease of the transmittance by up to 12.3 and 21.8% for ZnO and TiO_2 coatings, respectively.

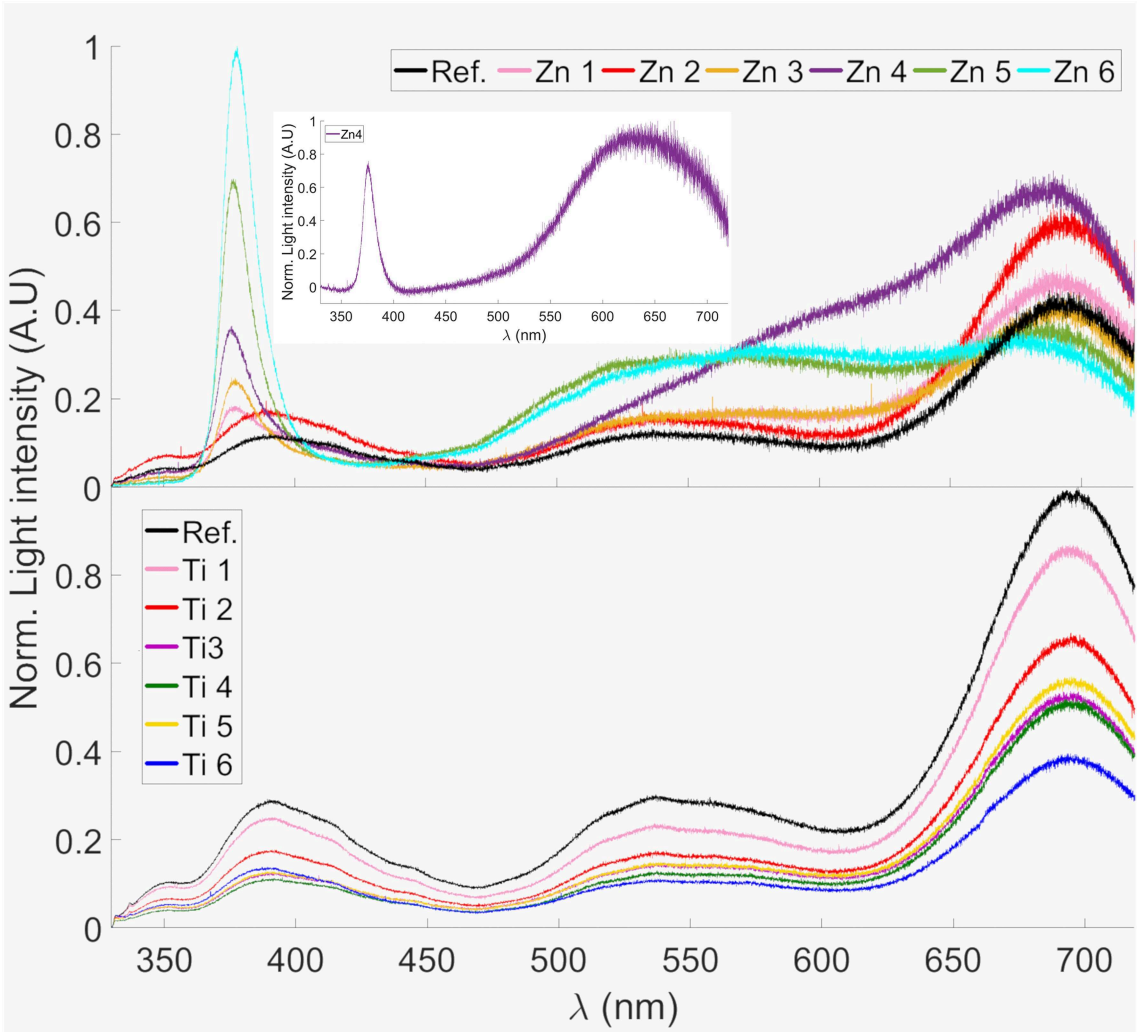

FIGURE 7 | Photoluminescence spectra of ZnO- and TiO_2-coated glass samples. The spectra were normalized to the highest peak. The inset shows the Zn4 photoluminescence spectra subtracted by the reference, clearly revealing the 640 nm emission peak.

Effect on Photoluminescence

Figure 7 shows the photoluminescence spectra between 330 and 720 nm of the ZnO- and TiO_2-coated glass substrates. All samples as well as the reference shows a distinct peak around 695 nm. This can probably be attributed to the Fe^{3+} present in the glass since it has shown a peak in photoluminescence at wavelengths around 700 nm when present in silicate glass (Bingham et al., 2007). The reference sample also shows a peak at 390 nm, this could be due to photoluminescence from SiO_2 (Nagata et al., 2004).

All Zn-samples, except Zn2, possess a strong narrow emission peak that can be observed at approximately 377 nm, which is not present in the reference sample. This corresponds well to the photoluminescence observed in ZnO nanorods by Wu et al. (2006) and which can be attributed to a common excitation recombination of ZnO (Studenikin et al., 1998; Kong et al., 2001). The 377 nm PL emission can be an explanation for the sensitization of Fe^{3+} absorption at 320–380 nm, c.f. **Figure 6**. Sample Zn4 shows a different pattern compared to the reference and the other coated samples in the wavelength interval 550–650 nm. When the photoluminescence from the reference sample was subtracted from sample 4, a peak at 640 nm could be distinguished; this is shown in the inset of **Figure 7**. This also corresponds well to the photoluminescence observed for ZnO nanorods (Wu et al., 2006), which was also observed by Studenikin et al. (1998) and has been attributed to oxygen interstitial defects in ZnO, i.e., over-stoichiometric ZnO. The opposite, under-stoichiometric ZnO, is indicated to give a green emission at about 510 nm.

The effect that our deposited ZnO and TiO_2 thin films have on the photoluminescence emission makes us confident that these thin films are mostly amorphous. The photoluminescent bands that we interpret as defects and the Fe^{3+} sensitization emissions for the samples are strong and dominate the photoluminescence spectra, see **Figure 7**. For the ZnO-coated samples it is despite that similar literature data, but with somewhat different experimental circumstances, refer to the ZnO films as mostly

crystalline (Kamata et al., 1994; Hosseinmardi et al., 2012; Villegas et al., 2018).

Discussion of the Effect for PV Modules

We have shown that UV blocking can be achieved with the cost of reducing the transmittance. Specifically, there was a 75.7% transmittance and a simultaneous reduction of 83.4% integrated transmittance for the sample Zn4, c.f. **Table 3**. This opens the possibility for maintaining UV protection and gaining useful energy for the PV by lowering the Fe_2O_3 content in the glass without compromising the service lifetime of the PV module. The energy balance for transmitted and useful light for PV modules will be possible to model and optimize in future studies based on information as for instance possible limits for Fe_2O_3 content, cost and efficiency. Furthermore, photon energy down-conversion, i.e., photoluminescence, can be an advantage and a route to utilizing UV light while still not exposing the PV cells to UV light. As for disadvantages, we can list higher reflectivity and scattering. If the surface coating is properly structured, it might not be a serious disadvantage or perhaps even an advantage (Brongersma et al., 2014), as the diffused light contains in fact more photons than the direct light of normal incidence. This is especially valid for façade-applied PV modules where there is in fact very little solar radiation of normal incidence. Another parameter not previously mentioned is the factor of heat. A photon's energy that is not converted into electricity is transformed into heat that in fact lowers the efficiency of the PV module. Beyond the scope of the current paper we would also like to draw the attention to making crystalline ZnO or TiO_2 coatings having similar beneficial properties but with the added value of photocatalysis (Gao and Nagai, 2006; He et al., 2012) and hydrophilic behavior with UV exposure (Watanabe et al., 1999; Sun et al., 2001), thereby giving PV-covered glasses reduced maintenance. Doped ZnO also offers another dimension as a transparent conductive coating offering possible IR reflection for wavelengths non-convertible to energy for PV modules (Deubener et al., 2009).

CONCLUSIONS

Glass coated with ZnO showed a trend to shift the UV-cutoff to longer wavelength as well as lowering the optical band gap of the coated glass sample. The major reason for this is likely to be caused by tetrahedrally coordinated Fe^{3+} having an absorption peak at about 380 nm but also being sensitized by the presence of the ZnO coating. Such a trend is less clear for the samples coated with TiO_2. Both sample series showed a significant increase in total reflection for the normal incident light due to the higher refractive index of the thin film oxide coatings. However, the increase in diffuse reflection was significantly lower, <4%; this is an advantage for application on the cover glass of PV-modules where most of the incoming light will be of diffuse character.

The coated glass showed a potential improvement in life expectancy of PV modules through a decrease of destructive UV-radiation transmission to the encapsulant up to a relative 36.0% and 54.3% for TiO_2 and ZnO, coatings, respectively. Additionally, although the coated samples have shown a relative transmission reduction at the useful spectral region up to 21.8 and 12.3% for TiO_2 and ZnO coatings, respectively, the transmissivity degradation of the encapsulant should be effectively prevented. For ZnO it is evident that the Fe^{3+} content plays an important role for the UV-blocking activity, which would be a tradeoff between limiting the glass's iron content while still having enough UV protection. Furthermore, ZnO-coated glass also showed potential regarding down conversion of UV light to visible wavelength with peaks at 377 and 640 nm. Thus, ZnO is feasible to be investigated for application as coating to cover glasses of PV modules but must be optimized as there is a tradeoff between UV-blocking and transmittance in the useful spectral region for PV modules.

AUTHOR CONTRIBUTIONS

SK perceived the idea of the paper. WJ performed the thin film deposition and photoluminescence measurements with the guidance of SK, BJ, and LÖ. AP performed the UV-VIS spectroscopy measurements with guidance from SA. SA performed the AFM measurements. WJ and AP evaluated the results of the measurements. WJ and SK wrote the draft of the paper. All authors were involved in the discussions and elaborating the final manuscript text.

ACKNOWLEDGMENTS

Jakob Thyr at the Ångström Laboratory, Uppsala University was greatly acknowledged for his supervision during the photoluminescence measurements.

REFERENCES

Abou-Helal, M. O., and Seeber, W. T. (2002). Preparation of TiO_2 thin films by spray pyrolysis to be used as a photocatalyst. *Appl. Surf. Sci.* 195, 53–62. doi: 10.1016/S0169-4332(02)00533-0

Allsopp, B. L., Christopoulou, G., Brookfield, A., Forder, S. D., and Bingham, P. A. (2018). Optical and structural properties of d^0 ion-doped silicate glasses for photovoltaic applications. *Phys. Chem. Glasses Euro. J. Glass Sci. Technol. B* 59, 193–202. doi: 10.13036/17533562.59.4.003

Bamford, C. R. (1982). Optical properties of flat glass. *J. Non Cryst. Solids* 47, 1–20. doi: 10.1016/0022-3093(82)90342-8

Bingham, P. A., Parker, J. M., Searle, T. M., and Smith, I. (2007). Local structure and medium range ordering of tetrahedrally coordinated Fe^{3+} ions in alkali–alkaline earth–silica glasses. *J. Non-Crystalline Solids* 353, 2479–2494. doi: 10.1016/j.jnoncrysol.2007.03.017

Brongersma, M. L., Cui, Y., and Fan, S. (2014). Light management for photovoltaics using high-index nanostructures. *Nat. Mater.* 13, 451–460. doi: 10.1038/nmat3921

Brow, R. K., and Schmitt, M. L. (2009). A survey of energy and environmental applications of glass. *J. Eur. Ceram. Soc.* 29, 1193–1201. doi: 10.1016/j.jeurceramsoc.2008.08.011

Burrows, K., and Fthenakis, V. (2015). Glass needs for a growing photovoltaics industry. *Solar Energy Mater. Solar Cells* 132, 455–459. doi: 10.1016/j.solmat.2014.09.028

Czanderna, A. W., and Pern, F. J. (1996). Encapsulation of PV modules using ethylene vinyl acetate copolymer as a pottant: a critical review.

Solar Energy Mater. Solar Cells 43, 101–181. doi: 10.1016/0927-0248(95)00150-6

Daneo, A. G., Falcone, R., and Hreglich, S. (2009). Effect of the redox state on container glass colour stability. *Glass Technol. Euro. J. Glass Sci. Technol. A* 50, 147–150. Available online at: https://www.ingentaconnect.com/content/sgt/gta/2009/00000050/00000003/art00004

Deubener, J., Helsch, G., Moiseev, A., and Bornhöft, H. (2009). Glasses for solar energy conversion systems. *J. Eur. Ceram. Soc.* 29, 1203–1210. doi: 10.1016/j.jeurceramsoc.2008.08.009

Dhar, S., Roy Barman, A., Rusydi, A., Gopinadhan, K., Feng, Y., Breese, M., et al. et al. (2013). "Effect of Ta alloying on the optical, electronic, and magnetic properties of TiO_2 thin films," in *Functional Metal Oxides: New Science and Novel Applications,* eds S. B. Ogale, T. V. Venkatesan, and M. G. Blamire (Weinheim: Wiley-VCH Verlag GmbH & Co), 133–162. doi: 10.1002/9783527654864.ch4

Gao, Y., and Nagai, M. (2006). Morphology evolution of ZnO thin films from aqueous solutions and their application to solar cells. *Langmuir* 22, 3936–3940. doi: 10.1021/la053042f

Goodyear, J. K., and Lindberg, V. L. (1980). Low absorption float glass for back surface solar reflectors. *Solar Energy Mater.* 3, 57–67. doi: 10.1016/0165-1633(80)90049-0

He, H., Liu, C., Dubois, K. D., Jin, T., Louis, M. E., and Li, G. (2012). Enhanced charge separation in nanostructured TiO_2 materials for photocatalytic and photovoltaic applications. *Ind. Eng. Chem. Res.* 51, 11841–11849. doi: 10.1021/ie300510n

Hosseinmardi, A., Shojaee, N., Keyanpour-Rad, M., and Ebadzadeh, T. (2012). A study on the photoluminescence properties of electrospray deposited amorphous and crystalline nanostructured ZnO thin films. *Ceramics Int.* 38, 1975–1980. doi: 10.1016/j.ceramint.2011.10.031

IEA (2011). *Solar Energy Perspectives.* Paris: International Energy Agency.

IPCC (2014). "Summary for policymakers," in *Climate Change 2014: Mitigation of Climate Change. Contribution of Working Group III to the Fifth Assessment Report of the Intergovernmental Panel on Climate Change,* eds O. Edenhofer, R. Pichs-Madruga, Y. Sokona, E. Farahani, S. Kadner, K. Seyboth, A. Adler, I. Baum, S. Brunner, P. Eickemeier, B. Kriemann, J. Savolainen, S. Schlömer, C. von Stechow, T. Zwickel, and J. C. Minx (Cambridge, UK; New York, NY: Cambridge University Press).

Jellison, G. E., and Boatner, L. A. (1998). Optical functions of uniaxial ZnO determined by generalized ellipsometry. *Phys. Rev. B* 58, 3586–3589. doi: 10.1103/PhysRevB.58.3586

Jellison, G. E., Modine, F. A., and Boatner, L. A. (1997). Measurement of the optical functions of uniaxial materials by two-modulator generalized ellipsometry: rutile (TiO_2). *Opt. Lett.* 22, 1808–1810. doi: 10.1364/OL.22.001808

Jordan, D. C., and Kurtz, S. R. (2013). Photovoltaic degradation rates—an analytical review. *Prog. Photovoltaics Res. Appl.* 21, 12–29. doi: 10.1002/pip.1182

Kamata, K., Nishino, J., Ohshio, S., Maruyama, K., and Ohtuki, M. (1994). Rapid formation of zinc oxide films by an atmospheric-pressure chemical vapor deposition method. *J. Am. Ceramic Soc.* 77, 505–508. doi: 10.1111/j.1151-2916.1994.tb07021.x

Karlsson, S., and Wondraczek, L. (2019). "Strengthening of Oxide Glasses," in *Encyclopedia for Glass Science, Technology, History and Culture*, ed P. Richet (Hoboken, NJ: John Wiley & Sons Inc.).

Kong, Y. C., Yu, D. P., Zhang, B., Fang, W., and Feng, S. Q. (2001). Ultraviolet-emitting ZnO nanowires synthesized by a physical vapor deposition approach. *Appl. Phys. Lett.* 78, 407–409. doi: 10.1063/1.1342050

Kuitche, J. M., Pan, R., and TamizhMani, G. (2014). Investigation of dominant failure mode(s) for field-aged crystalline silicon PV modules under desert climatic conditions. *IEEE J. Photovoltaics* 4, 814–826. doi: 10.1109/JPHOTOV.2014.2308720

Lee, G. H., Kawazoe, T., and Ohtsu, M. (2002). Difference in optical bandgap between zinc-blende and wurtzite ZnO structure formed on sapphire (0001) substrate. *Solid State Commun.* 124, 163–165. doi: 10.1016/S0038-1098(02)00537-9

Masson, G., Kaizuka, I., and Cambiè, C. (2018). *IEA Report PVPS: A Snapshot of Global PV (1992-2017).* International Energy Agency.

Nagata, S., Yamamoto, S., Toh, K., Tsuchiya, B., Ohtsu, N., Shikama, T., et al. (2004). Luminescence in SiO_2 induced by MeV energy proton irradiation. *J. Nuclear Mater.* 329–333, 1507–1510. doi: 10.1016/j.jnucmat.2004.04.242

Nielsen, K. H., Orzol, D. K., Koynov, S., Carney, S., Hultstein, E., and Wondraczek, L. (2014). Large area, low cost anti-reflective coating for solar glasses. *Solar Energy Mater. Solar Cells* 128, 283–288. doi: 10.1016/j.solmat.2014.05.034

Okuya, M., Prokudina, N. A., Mushika, K., and Kaneko, S. (1999). TiO_2 thin films synthesized by the spray pyrolysis deposition (SPD) technique. *J. Eur. Ceram. Soc.* 19, 903–906. doi: 10.1016/S0955-2219(98)00341-0

Oliveira, M. C. C. D., Diniz Cardoso, A. S. A., Viana, M. M., and Lins, V.,d.F.C. (2018). The causes and effects of degradation of encapsulant ethylene vinyl acetate copolymer (EVA) in crystalline silicon photovoltaic modules: A review. *Renew. Sust. Energy Rev.* 81, 2299–2317. doi: 10.1016/j.rser.2017.06.039

Osterwald, C. R., Benner, J. P., Pruett, J., Anderberg, A., Rummel, S., and Ottoson, L. (2003). "Degradation in weathered crystalline-silicon PV modules apparently caused by UV radiation," in *3rd World Conference on Photovoltaic Energy Conversion* (Osaka).

Perednis, D., and Gauckler, L. J. (2005). Thin film deposition using spray pyrolysis. *J. Electroceramics* 14, 103–111. doi: 10.1007/s10832-005-0870-x

Roos, A. (1993). Use of an integrating sphere in solar energy research. *Solar Energy Mater. Solar Cells* 30, 77–94. doi: 10.1016/0927-0248(93)90033-Y

Rouxel, T., Sellappan, P., Celarie, F., Houizot, P., and Sangleboeuf, J. C. (2014). Toward glasses with better indentation cracking resistance. *Cr Mecanique* 342, 46–51. doi: 10.1016/j.crme.2013.10.008

Rubin, M. (1985). Optical properties of soda lime silica glasses. *Solar Energy Mater.* 12, 275–288. doi: 10.1016/0165-1633(85)90052-8

Schröder, A. (1928). XXXV. Beiträge zur Kenntnis des Feinbaues des Brookits und des physikalischen Verhaltens sowie derZustandsänderungen der drei natürlichen Titandioxyde. *Z. Kristallograph.* 67:485. doi: 10.1524/zkri.1928.67.1.485

Shannon, R. D., Shannon, R. C., Medenbach, O., and Fischer, R. X. (2002). Refractive index and dispersion of fluorides and oxides. *J. Phys. Chem. Ref. Data* 31, 931–970. doi: 10.1063/1.1497384

Studenikin, S. A., Golego, N., and Cocivera, M. (1998). Fabrication of green and orange photoluminescent, undoped ZnO films using spray pyrolysis. *J. Appl. Phys.* 84, 2287–2294. doi: 10.1063/1.368295

Sun, R.-D., Nakajima, A., Fujishima, A., Watanabe, T., and Hashimoto, K. (2001). Photoinduced Surface Wettability Conversion of ZnO and TiO_2 Thin Films. *J. Phys. Chem. B* 105, 1984–1990. doi: 10.1021/jp002525j

Sundberg, P., Grund Bäck, L., Orman, R., Booth, J., and Karlsson, S. (2019). Simultaneous chemical vapor deposition and thermal strengthening of glass. *Thin Solid Films* 669, 487–493. doi: 10.1016/j.tsf.2018.11.028

Tauc, J. (1968). Optical properties and electronic structure of amorphous Ge and Si. *Mater. Res. Bull.* 3, 37–46. doi: 10.1016/0025-5408(68)90023-8

Villegas, E. A., Aldao, C. M., Savu, R., Ramajo, L. A., and Parra, R. (2018). Effects of grain size on the UV-photoresponse of zinc oxide thin films grown by spray-pyrolysis. *Phys. Status Solidi a* 215:1800107. doi: 10.1002/pssa.201800107

Volotinen, T. T., Parker, J. M., and Bingham, P. A. (2008). Concentrations and site partitioning of Fe^{2+} and Fe^{3+} ions in a soda-lime-silica glass obtained by optical absorbance spectroscopy. *Phys. Chem. Glasses Euro. J. Glass Sci. Technol. B* 49, 258–270. Available online at: https://www.ingentaconnect.com/content/sgt/ejgst/2008/00000049/00000005/art00004

Watanabe, T., Nakajima, A., Wang, R., Minabe, M., Koizumi, S., Fujishima, A., et al. (1999). Photocatalytic activity and photoinduced hydrophilicity of titanium dioxide coated glass. *Thin Solid Films* 351, 260–263. doi: 10.1016/S0040-6090(99)00205-9

Wondraczek, L., Mauro, J. C., Eckert, J., Kühn, U., Horbach, J., Deubener, J., et al. (2011). Towards ultrastrong glasses. *Adv. Mater.* 23, 4578–4586. doi: 10.1002/adma.201102795

Wu, L., Wu, Y., Pan, X., and Kong, F. (2006). Synthesis of ZnO nanorod and the annealing effect on its photoluminescence property. *Opt. Mater.* 28, 418–422. doi: 10.1016/j.optmat.2005.03.007

Conflict of Interest: The authors declare that the research was conducted in the absence of any commercial or financial relationships that could be construed as a potential conflict of interest.